Study on chemical compounds for the development of anti-ebolavirus drugs

（抗エボラウイルス薬開発に向けた化合物の探索）

Mao ISONO

Contents

Abbreviations

BDBV	Bundibugyo virus
BOMV	Bombali virus
BSA	bovine serum albumin
CMC	carboxymethyl cellulose
CT	cytoplasmic tail
DAPI	4′,6-diamidino-2-phenylindole, dihydrochloride
DDI	Drug Development Initiative
DiI	1,1′-dioctadecyl-3,3,3′,3′-tetramethylindocarbocyanine perchlorate
DMEM	Dulbecco's modified Eagle's medium
DMSO	dimethyl sulfoxide
DRC	Democratic Republic of Congo
EBOV	Ebola virus
EBOV-GFP	recombinant EBOV encoding GFP
ELISA	enzyme-linked immunosorbent assay
ESCRT	endosomal sorting complex required for transport
EVD	Ebola virus disease
FCS	fetal calf serum
FDA	Food and Drug Administration
GFP	green fluorescent protein
GP	glycoprotein
HEK	human embryonic kidney
HRP	horseradish peroxidase

IFL	internal fusion loop
ITbM	Institute of Transformative Bio-Molecules
IUs	infectious units
MARV	Marburg virus
MEM	Eagle's minimal essential medium
MLD	mucin-like domain
NC	negative control
NP	nucleoprotein
NPC1	Niemann-Pick C1
OD	optical density
PBS	phosphate-buffered saline
PBST	0.05% Tween 20 in PBS
PC	positive control
PFU	plaque forming units
RdRp	RNA-dependent RNA polymerase
RESTV	Reston virus
RNP	ribonucleoprotein
RT	room temperature
rVSV-EBOV	replication-competent recombinant VSV
SERM	selective estrogen receptor modulators
SUDV	Sudan virus
TAFV	Taï Forest virus
TIM-1	T-cell immunoglobulin and mucin domain 1
TM	transmembrane region

TMB	3,3',5,5'-tetramethyl-benzidine
Vero E6/eGFP-Rab7	eGFP-Rab7-expressing Vero E6
Vero E6/NPC1-KO	NPC1-knockout Vero E6
VLP	virus-like particle
VP	viral protein
VSV	vesicular stomatitis virus

Preface

Ebolaviruses and Marburgvirus belong to the family *Filoviridae* in the order *Mononegavirales* consisting of viruses that have nonsegmented negative-stranded RNA genomes. The genus *Ebolavirus* contains six species: *Zaire ebolavirus*, *Bundibugyo ebolavirus*, *Taï Forest ebolavirus*, *Sudan ebolavirus*, *Reston ebolavirus*, and *Bombali ebolavirus* represented by Ebola virus (EBOV), Bundibugyo virus (BDBV), Taï Forest virus (TAFV), Sudan virus (SUDV), Reston virus (RESTV), and Bombali virus (BOMV), respectively[1,2]. On the other hand, the genus *Marburgvirus* contains only one species: *Marburg Marburgvirus* including Marburg virus (MARV) and Ravn virus. These filoviruses, with the exception of RESTV and BOMV, are known to cause severe hemorrhagic fever in humans[3,4] The case fatality rate is up to about 90% but varies among virus species and even variants[5].

Ebolaviruses have caused sporadic outbreaks of Ebola virus disease (EVD) in Africa. In 2013-16, the unprecedented scale of the EVD outbreak occurred in the West African countries and it spread to other areas including United States and some European countries, demonstrating that EVD has a potential to become a worldwide public health concern. The second largest outbreak in 2018-20[6–8] and the latest outbreak in 2020 of EVD[9] occurred in Democratic Republic of Congo (DRC). Although several candidate drugs were clinically tested during the EVD outbreaks, only one drug, which is a therapeutic monoclonal antibody cocktail, Inmazeb, has been approved by United States Food and Drug Administration (FDA)[10]. Due to the shortage of medicines, more treatment options for EVD are urgently needed.

The ebolavirus RNA genome encodes at least 7 structural proteins, nucleoprotein (NP), polymerase cofactor VP35, matrix protein VP40, envelope

glycoprotein (GP), transcriptional activator VP30, nucleocapsid-associated protein VP24, and RNA-dependent RNA polymerase L. GP forms spikes on the virion surface and responsible for receptor binding and membrane fusion[11,12]. The interaction between GP and host cell receptors such as C-type lectins and T-cell immunoglobulin and mucin domain 1 (TIM-1) regulated the entry of ebolaviruses into host cells[13–15]. The virion is then internalized into endosomes by clathrin-mediated macropinocytosis[16–18]. In endosomes, GP is proteolytically processed by host proteases like cathepsins B and L in a low pH environment[19]. The partially digested GP interacts with the endosomal fusion receptor, Niemann-Pick C1 (NPC1), and subsequently fusion between the viral envelope and the endosomal membrane occurs, leading to the release of the viral ribonucleoprotein (RNP) complex into cytoplasm[20,21]. The RNP complex is formed by the genomic RNA, NP, VP24, VP35, VP30, and L and responsible for viral RNA transcription and replication. EBOV VP35 and VP24 are known interferon antagonists[22,23]. VP40, the matrix protein, is the most abundant protein in the virus particle and plays a key role in the budding from infected cells[24,25].

In this study, it was investigated that chemical compounds for the development of anti-ebolavirus drugs using small compound libraries of university of Tokyo and Nagoya university, focusing on multiple steps of the virus replication (i.e., entry into cells, genome transcription/replication, and budding from cells). In chapter I, the efficiency and inhibition mechanism of HUP2976, a novel entry inhibitor against EBOV, was examined. In chapter II, a single assay that was based on an EBOV minigenome reporter assay and a virus-like particles (VLPs) formation assay was established. I screened a small compound library (approximately 20,000 compounds) and discovered several compounds that might have potential as candidates of EBOV replication or/and budding inhibitors.

Chapter I:

A biaryl sulfonamide derivative as a novel inhibitor of filovirus infection

Introduction

EBOV caused the largest outbreak of EVD in 2013-2016 in West Africa, with over 28,000 cases and 11,000 deaths. In the second largest EVD outbreak in the DRC, declared by the Ministry of Health of the DRC on 1st August 2018, a total of 3,481 EVD confirmed and probable cases and 2,299 deaths have been reported (as of July 3, 2020)[5,7,8]. Clinical trials of antibody therapies (i.e., ZMapp, REGN-EB3, and mAb114) were conducted during the outbreaks in West Africa and the DRC[26,27]. Several small compound candidates for treatment of EVD such as T-705 (favipiravir), and GS-5734 (remdesivir), all of which are nucleotide analogues, have also been tested in animal models and clinical cases[28–30]. In particular, remdesivir was experimentally used for infected patients in the DRC[31]. However, none of the previously developed chemical compounds have been approved as anti-EVD drugs, although a monoclonal antibody cocktail, Inmazeb, that inhibits EBOV entry into cells has been approved by FDA.

The viral surface GP is responsible for the entry step including receptor binding and membrane fusion[11,12]. After attachment, virions are captured by clathrin-mediated macropinocytosis into endosomes[16,32]. Following acidification of the endosome, host proteases such as cathepsin B/L cleave GP into the fusion-active form. Cleaved GP is able to interacts with the host endosomal receptor NPC1 to trigger fusion of the viral and endosomal membranes[20,21,33], followed by release of RNP complexes into the cytoplasm. The process from virion attachment to membrane fusion is a critical step to infect host cells. Hence, it has been thought that the entry process is an effective target to develop

therapeutics against EVD. Indeed, some leading drug candidates are therapeutic antibodies which inhibit the cellular entry of EBOV.

In this study, a biaryl sulfonamide derivative that specifically inhibits the entry of filoviruses into target cells was discovered via screening using pseudotyped VSV with filovirus GPs. HUP2976 was selected as a potent entry inhibitor of filovirus infection after investigating characters of this compound such as efficacy, cytotoxicity and so on. I determined the inhibitory mechanism of this drug candidate by monitoring each step of the viral entry process (attachment, internalization, and membrane fusion) using VLPs consisting of EBOV NP, VP40, and GP. HUP2976 efficiently blocked the membrane fusion in cellular endosomes, though it did not inhibit VLP binding to the NPC1 receptor, suggesting that the mechanism of action of HUP2976 was fusion inhibition independent from the GP-NPC1 engagement.

Materials and Methods

Cells and cellular assays. Human embryonic kidney (HEK) 293T, African green monkey kidney Vero E6, NPC1-knockout Vero E6 (Vero E6/NPC1-KO)[34], eGFP-Rab7-expressing Vero E6 (Vero E6/eGFP-Rab7) kindly provided by Dr. A. Nanbo, Nagasaki University, Japan, and human hepatoma Huh7 cells were grown in Dulbecco's modified Eagle's medium (DMEM) (Sigma) supplemented with 10% fetal calf serum (FCS) (Cell Culture Bioscience), 100 U/ml penicillin, and 0.1 mg/ml streptomycin (Gibco). Cell viabilities were measured with the alamar blue assay (Biosource International) according to the manufacturer's instructions using dimethyl sulfoxide (DMSO) as a negative control. Endosomal pH in Vero E6/eGFP-Rab7 was tested using LysoTracker Red DND-99 (Life Technologies).

Vesicular stomatitis virus (VSV) pseudotyped with filovirus GPs. The expression plasmids for filovirus GPs were constructed as described previously[12]. Mutant GP genes were constructed by site-directed mutagenesis with KOD-Plus Neo (Toyobo). Using VSV containing the green fluorescent protein (GFP) gene instead of the VSV glycoprotein (G) gene (VSVΔG*-G), GP-expressing plasmids, and HEK293T cells, replication-incompetent VSVs pseudotyped with ebolavirus and marburgvirus GPs were generated as described previously[12,35]. VSVs pseudotyped with GPs of EBOV (Mayinga), BDBV (Butalya), TAFV (Pauléoula), SUDV (Boniface), RESTV (Pennsylvania), and MARV (Angola) were preincubated with an anti-VSV G monoclonal antibody, VSV-G [N] 1-9, to abolish the background infectivity of parental VSVΔG*-G[36]. For virus titration, 10-fold serial dilutions of pseudotyped VSVs were inoculated into confluent monolayers of Vero E6 cells cultured on 96-well plates, and infectious units (IUs) were determined 18

hr later by counting the number of GFP-expressing cells with IN Cell Analyzer (GE Healthcare).

Replication-competent recombinant VSV (rVSV-EBOV) was generated as described previously[37] and its titer was determined by a conventional plaque assay. Briefly, Vero E6 cells were seeded on 12-well plates (3.0×10^5 cells/well) and incubated in a 5% CO_2 incubator at 37˚C for 18 hr. After aspirating the medium, serial dilutions (10-fold) of rVSV-EBOV were inoculated (100 μl/well) onto the cells. After incubation in a 5% CO_2 incubator at 37˚C for 1 hr with rocking every 15 min, the inoculum was removed and cells were washed with FCS free-DMEM. Following this, they were overlaid with Eagle's minimal essential medium (MEM) (Invitrogen) containing 1.0% Bacto Agar (BD), 0.3% bovine serum albumin (BSA) (Sigma), 100 U/ml penicillin, and 0.1 mg/ml streptomycin, and then incubated in 5% CO_2 incubator at 37˚C for 48 hr. Numbers of plaques at appropriate dilutions were counted to determine plaque forming units (PFU). The use of VSVs was approved by the Committee for Safety Management of Pathogens, Research Center for Zoonosis Control, Hokkaido University (10[06]). The generation of recombinant VSVs and plasmids was approved by the Ministry of Education, Culture, Sports, Science, and Technology, Japan and Hokkaido University Safety Committee for Genetic Recombination Experiments (21[4]).

Recombinant EBOV. Recombinant EBOV encoding GFP (EBOV-GFP) was generated as described previously[38]. EBOV-GFP was inoculated onto confluent monolayers of Vero E6 cells and incubated for 1 hr. Then the inoculum was removed and a 1.2% carboxymethyl cellulose (CMC)/MEM solution was added. Following incubation for 2-3 days at 37˚C, images were captured by fluorescent microscopy and numbers of GFP-

expressing foci were counted. All infectious work with EBOV-GFP was performed in the biosafety level-4 laboratory at the Integrated Research Facility of the Rocky Mountain Laboratories, Division of Intramural Research, National Institute of Allergy and Infectious Diseases, National Institutes of Health, Hamilton, Montana, USA. All standard operating procedures were approved by the Institutional Biosafety Committee.

Screening of the compounds. A chemical compound library consisting of 9,600 compounds was provided by the Drug Development Initiative (DDI), University of Tokyo. Vero E6 cells were seeded on 96-well plates (3.0×10^4 cells/well) and incubated for 18 hr. Then equal volumes of VSVs pseudotyped with filovirus GPs (1000 IUs/ml) diluted in DMEM with 2% FCS and P/S and chemical compounds (10 μM) were mixed, and added to the Vero E6 cells (100 μl/well). After 18 hr incubation in a 5% CO_2 incubator at 37˚C, GFP-expressing cells were counted using IN Cell Analyzer (GE Healthcare).

DiI assay. VLPs containing EBOV GP, VP40, and NP were purified as described previously[16,39]. VLPs were labeled with a lipophilic tracer, 1,1′-dioctadecyl-3,3,3′,3′-tetramethylindocarbocyanine perchlorate (DiI) (Invitrogen) at room temperature (RT) with gentle rocking in the dark for 1 hr. Labeled VLPs were diluted with phosphate-buffered saline (PBS) to 1 μg/ml. Vero E6/eGFP-Rab7 cells (1.5×10^5 cells/well) were cultured in 8-well chamber slides (Merck). Then they were washed with 250 μl of FCS-free DMEM and incubated with DiI-labelled VLPs on ice for 30 min. The cells were washed with FCS-free DMEM to remove unbound VLPs and incubated with 250 μl of DMEM containing HUP2976 (25 μM) for 0, 2, and 6 hr at 37°C to analyze attachment, internalization, and membrane fusion, respectively. In this assay, the fluorescent signal is

enhanced once the DiI-labelled VLP envelope fuses with the endosomal membrane[16]. To count the number of DiI-labelled VLPs, the cells were fixed with 4% paraformaldehyde for 15 min at RT. Then nuclei were stained with 1 μg/ml 4′,6-diamidino-2-phenylindole, dihydrochloride (DAPI) for 10 min at RT. Images were captured with a 63× oil objective lens using a Zeiss LSM780 inverted microscope and a ZEN 2010 software. Images of 4-20 optical sections were acquired in 0.5-1.0 μm steps to analyze the number of DiI-labeled VLPs (0 hr), the percentage of DiI-labeled VLPs that colocalized with eGFP-Rab7 (2 hr), and relative sizes and intensities of DiI dots (6 hr). Quantitative analyses were conducted with Image J software (NIH, USA).

GP-NPC1 binding assay. Vero E6/NPC1-KO cells and Vero E6/NPC1-KO cells expressing HA-tagged NPC1[34] were seeded in T-75 flasks. After harvesting with trypsin, the cells were sedimented at 1,000 rpm for 5 min. CHAPS-NTE buffer (0.5% wt/vol CHAPS, 140 mM NaC1, 10 mM Tris-HC1, 1 mM EDTA; pH 7.5)[40] was added to cells to a final concentration of 10^7 cells/ml. Then, EDTA-free Complete Protease Inhibitor Cocktail (Roche) was added. The cells were sedimented at 10,000 × g for 10 min at 4˚C and the supernatant was harvested. VLPs (1 mg/ml in PBS) were treated with thermolysin (Sigma) at 37˚C for 30 min. The VLP solution was diluted at 1:10 with 0.05 M carbonate buffer (pH 9.6). Enzyme-linked immunosorbent assay (ELISA) plates (Nunc, Maxisorp) were coated with the diluted VLPs, and incubated at 4˚C overnight. The VLPs were removed and the plates were blocked with BSA (10 mg/ml in PBS) and incubated at RT for 2 hrs. Recombinant monoclonal antibody mAb114, which blocks binding of NPC1 to GP via interaction with the glycan cap and the inner chalice of GP, was generated as a positive control based on the sequence described previously using γ1HC, and κLC

vectors[41–43]. Serially diluted HUP2976 and mAb114 (in PBS) were mixed with cell lysates (diluted at 1:20 with CHAPS-NTE buffer) and incubated at RT for 10 min. After washing the plates with 0.05% Tween 20 in PBS (PBST), the mixture was added to each well and incubated at 4˚C overnight. After removal of the mixture, the plates were washed with PBST 3 times, and rat anti-HA antibody 3F10 (Sigma) diluted with PBST containing BSA (5 mg/ml) was added, followed by incubation at RT for 1 hr. After washing 3 times with PBST, horseradish peroxidase (HRP)-conjugated anti-rat IgG (H+L) (Jackson ImmunoResearch) was added to each well. After incubation at RT for 1 hr, the plates were extensively washed and a 3,3',5,5'-tetramethyl-benzidine (TMB) substrate (Sigma) was added, followed by incubation in the dark at RT for 30-60 min. The optical density (OD) value at 450 nm was measured after stopping the reaction with 1M phosphoric acid. The use of recombinant proteins was approved by Hokkaido University Safety Committee for Genetic Recombination Experiments (21[4]).

Selection of HUP2976 escape mutants. Tenfold serial dilutions of rVSV-EBOV (approximately 2.0×10^2 to 2.0×10^6 PFU/0.1 ml in FCS free-DMEM) were mixed with equal volumes of HUP2976 (20 μM in FCS free-DMEM) and incubated at RT for 1 hr, then inoculated onto confluent Vero E6 cells grown in 6-well tissue culture plates. After adsorption for 1 hr, the cells were overlaid with MEM (Invitrogen) containing 1.0% Bacto Agar (BD) and 20 μM HUP2976, and then incubated in a 5% CO_2 incubator at 37˚C for 48 hrs. Mutant viruses growing in the presence of HUP2976 were purified from single isolated plaques and propagated on Vero E6 cells. Viral RNAs were extracted from the supernatant, the nucleotide sequences of the GP genes of the parent viruses and the escape mutants were determined and the amino acid sequences were compared among the viruses.

Results

Inhibitory effect of HUP2976 against VSVs pseudotyped with filovirus GPs. Using VSV pseudotyped with EBOV GP, a total of 9,600 compounds from the DDI of the University of Tokyo were screened for antiviral effects (i.e., entry inhibitors), and I obtained a biaryl sulfonamide derivative that inhibited the virus entry into target cells. The structure-activity correlation of derivatives of this lead compound enabled us to improve the inhibitory activity and the cytotoxicity (data not shown) and, thus, a viable drug candidate, HUP2976 was obtained (Fig. 1A).

I found that HUP2976 efficiently inhibited infection by VSVs pseudotyped with filovirus GPs, but not VSV G in Vero E6 and Huh7 cells, suggesting the potential of HUP2976 to specifically inhibit the entry of filoviruses (Fig. 1B). Notably, VSV pseudotyped with EBOV or BDBV GPs was almost completely neutralized at 0.31 μM in both Vero E6 and Huh7 cells. Among ebolaviruses, HUP2976 showed the weakest effect on RESTV GP-mediated infection. Although HUP2976 showed less efficacy against VSV pseudotyped with MARV GP, it reduced the infectivity at 5 μM in both Vero E6 and Huh7 cells (Fig. 1B). The 50% inhibitory concentrations (IC_{50}) of HUP2976 for pseudotyped VSVs using Vero E6 cells were 0.086 μM (EBOV GP), 0.270 μM (SUDV GP), 0.307 μM (TAFV GP), 0.050 μM (BDBV GP), 1.117 μM (RESTV GP), and 4.79 μM (MARV GP). Regarding Huh7 cells, IC_{50} of HUP2976 for pseudotyped VSVs were 0.010 μM (EBOV GP), 0.020 μM (SUDV GP), 0.151 μM (TAFV GP), 0.010 μM (BDBV GP), 0.280 μM (RESTV GP), and 0.570 μM (MARV GP). Significant cytotoxicity was not observed in both cell lines except the highest concentration (80 μM) for Huh7 cells (Fig. 1C). Dose-dependent inhibitory effects of HUP2976 on EBOV entry were confirmed using infectious EBOV-GFP (Fig. 2). It was found that sizes of virus-infected

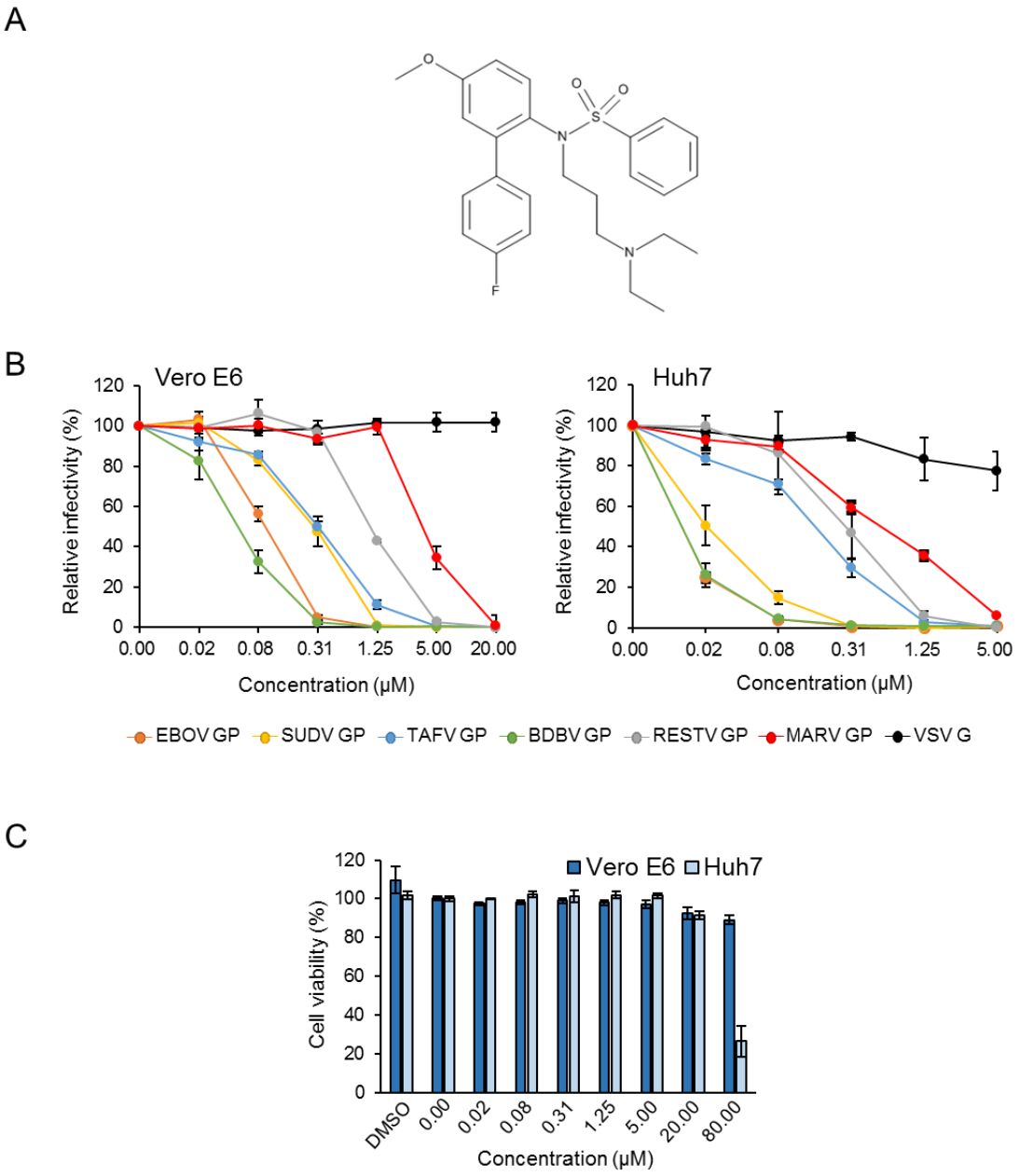

Fig. 1. HUP2976 and its inhibitory activity against VSVs pseudotyped with filovirus GPs. (A) Chemical structure of HUP2976 (MW: 470.6). (B) Pseudotyped VSVs (1,000 IU/ml) were mixed with equal volumes of HUP2976 and inoculated onto Vero E6 and Huh7 cells in 96-well plates. The cells were incubated at 37˚C for 18 hr and the numbers of GFP-expressing cells were counted using IN Cell Analyzer. One experiment performed in triplicate is shown; averages and standard deviations are presented. (C) Vero E6 and Huh7 cells were incubated with the indicated concentrations of HUP2976 or 0.8% DMSO. Cell viabilities were measured after 24 hour-incubation.

cell foci formed in the presence of HUP2976 were markedly smaller than in control cells treated with 0.5% DMSO, and that HUP2976 significantly reduced the number of visible foci formed by EBOV-GFP (Fig. 2).

Inhibition of fusion between virus and endosomal membrane by HUP2976. I then investigated the inhibitory effects of HUP2976 on viral attachment (0 hr), internalization (2 hr), and membrane fusion (6 hr) using DiI-labelled VLPs consisting of EBOV NP, VP40, and GP (Fig. 3). The number of VLPs attached to the surface of Vero E6 cells in the presence of HUP2976 was not significantly different from that of untreated (i.e., DMSO-treated) cells, indicating that HUP2976 did not interfere with VLP attachment (Fig. 3A, B). Likewise, the number of VLPs colocalizing with eGFP-Rab7, a late endosome marker, was similar for HUP2976-treated and untreated cells, suggesting that HUP2976 did not affect subsequent uptake of VLPs into cellular endosomes (Fig. 3C, D). Finally, membrane fusion efficiency was analyzed by detecting dequenched DiI fluorescence signals[16,44]. In this assay, when DiI-labeled VLP envelopes fuse with the endosomal membrane, enhanced fluorescent signals are observed. It was observed significantly increased DiI signals colocalizing with Rab7 in untreated cells, indicating that membrane fusion occurred efficiently in endosomes (Fig. 3E, F). In contrast, dequenched DiI signals were significantly reduced in the presence of HUP2976, indicating that HUP2976 prevented GP-mediated membrane fusion in endosomes (Fig. 3E, F). Using a LysoTracker marker, I examined endosomal acidification in the presence or absence of HUP2976 and found that this compound did not significantly raise the endosomal pH (Fig. 3G).

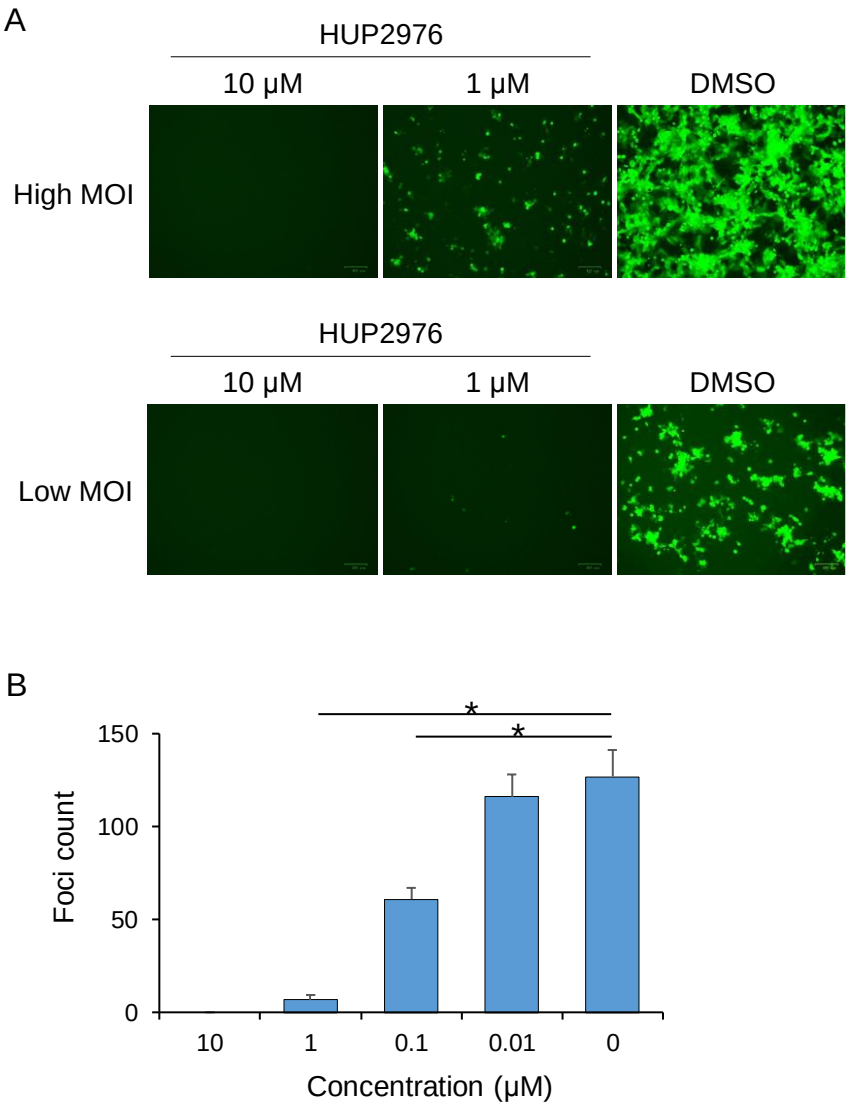

Fig. 2. Inhibitory activity of HUP2976 against EBOV-GFP. EBOV-GFP was diluted to infect Vero E6 cells at high (0.5-1.0) and low (0.05-0.1) multiplicities of infection. Following infection, the cells were incubated with the indicated concentrations of HUP2976 for 2 days and fluorescent images were captured (A). The numbers of GFP-expressing foci were counted from triplicate wells (low moi samples) and averages and standard deviations are shown (B). Statistical analysis was performed using Student's *t*-test (*$p < 0.05$).

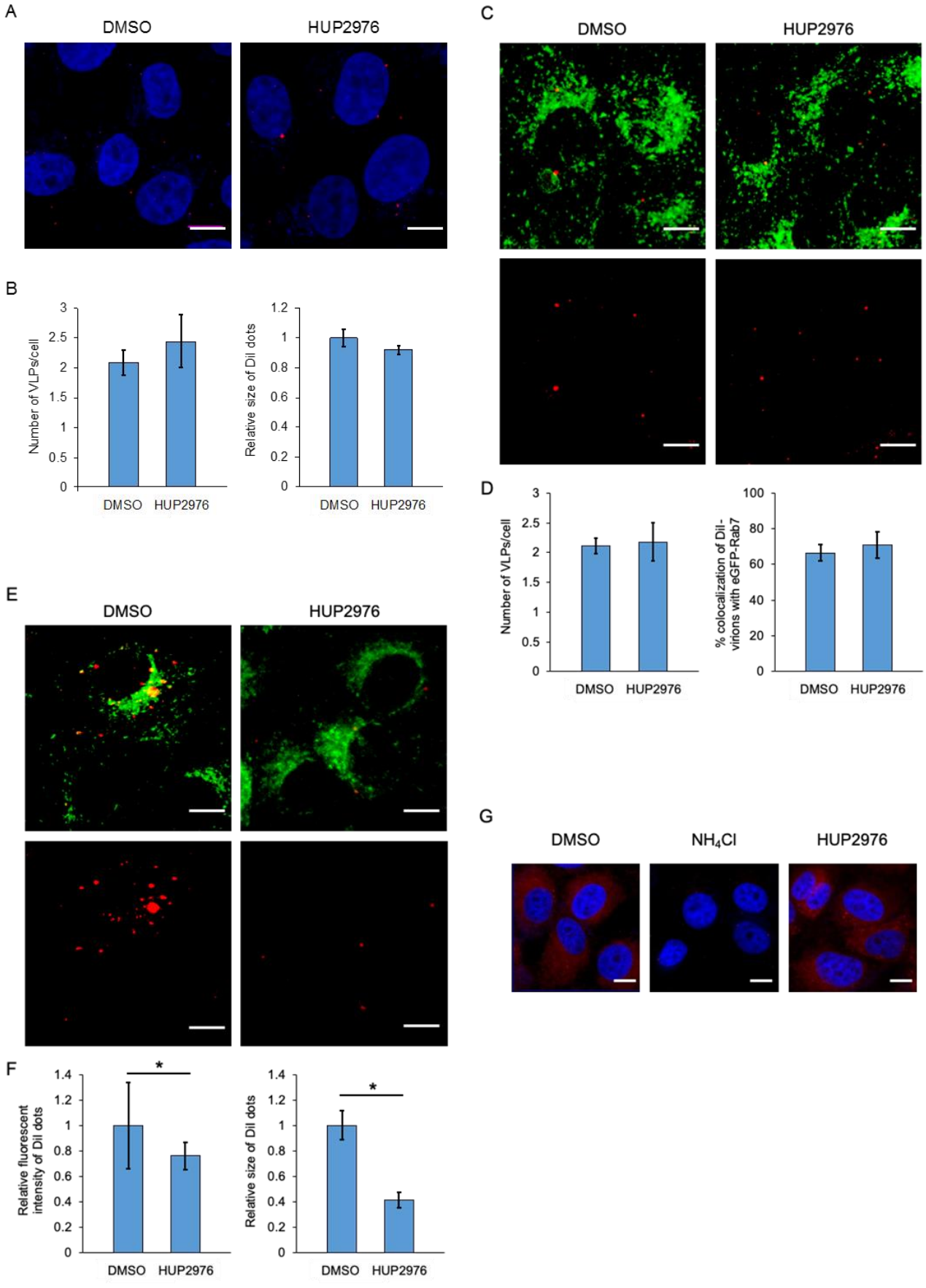
A
DMSO
HUP2976
B
Number of VLPs/cell
Relative size of Dil dots
DMSO
HUP2976
C
DMSO
HUP2976
D
Number of VLPs/cell
% colocalization of Dil-virions with eGFP-Rab7
DMSO
HUP2976
E
DMSO
HUP2976
F
Relative fluorescent intensity of Dil dots
Relative size of Dil dots
*
DMSO
HUP2976
G
DMSO
NH4Cl
HUP2976

Fig. 3. Membrane fusion inhibition by HUP2976. DiI-labelled VLPs (red) were inoculated into confluent Vero E6 cells expressing eGFP-Rab7 (green) and incubated for 30 min on ice. After adsorption, the cells were incubated for 0 (A,B), 2 (C,D), or 6 hrs (E,F) at 37˚C in the presence of HUP2976 (25 μM) or 0.25% DMSO. The cells were fixed with 4% paraformaldehyde and nuclei were stained with DAPI (blue). DiI signals on the cell surface and in the cytoplasm were monitored by confocal laser scanning microscopy (A,C,E). Scale bars represent 10 μm. (B,D,F) Three microscopic fields were acquired randomly, and the number of DiI-labeled virions was measured in approximately 50 individual cells (B,D). Percentage of colocalization (D) and size (B,F) and fluorescence intensity (F) of DiI dots were quantified using Image J software. Averages and standard deviations of three independent experiments are shown (B,D,F). Statistical analysis was performed using Student's *t*-test (*$p < 0.05$). (G) Vero E6/eGFP-Rab7 cells were incubated with HUP2976 (25 μM), NH_4Cl (25 mM), or DMSO (0.25%) and stained with LysoTracker Red DND-99. Acidic endosomes are viualized in red.

Effects of HUP2976 and mAb114 on EBOV GP-NPC1 binding. Since EBOV GP is known to bind the endosomal fusion receptor NPC1 to mediate membrane fusion, I conducted EBOV GP-NPC1 binding assays to examine whether the interaction between EBOV GP and NPC1 was inhibited by HUP2976. Consistent with a previous study[45], the positive control antibody mAb114, which binds to the NPC1 binding region of EBOV GP, inhibited the interaction of these molecules in a dose-dependent manner (Fig. 4). In contrast, HUP2976 did not reduce the binding activity of EBOV GP to NPC1 even at the highest concentration tested (Fig. 4). These results indicated that HUP2976 did not affect the interaction between EBOV GP and NPC1.

Amino acid substitutions in the EBOV GP escape mutants. To identify amino acid residues that could potentially interact with HUP2976, escape mutants were selected using replication-competent rVSV-EBOV. Six escape mutants were isolated and amino acid substitutions in the GP genes were analyzed (Fig. 5A). All the GP mutants had amino acid substitutions at positions 47 (Asp-to-Gly [1/6] or Asp-to-Glu [1/6]) or 66 (Val-to-Phe [4/6]), both of which are located in the base region (amino acid positions 33-70) of the GP molecule (Fig. 5B)[46].

After cloning these mutant GP genes into expression vectors, VSVs pseudotyped with mutant GPs were prepared to analyze whether these amino acid substitutions affected the inhibitory efficacy of HUP2976 (Fig. 5C). Single substitutions at position 47 and 66 similarly reduced the sensitivity of the virus to HUP2976 as indicated by approximately 60- to 100-fold increased IC_{50} values. There was no significant difference in the extent of the resistance among the mutants with single and double substitutions, indicating that either of the mutations at position 47 or 66 was sufficient to escape from

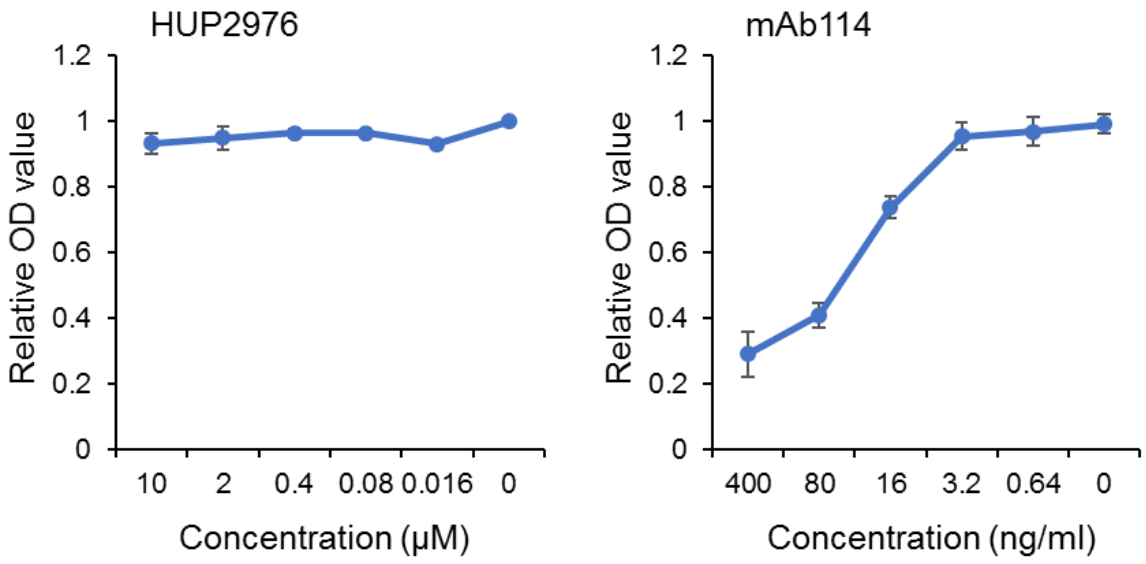

Fig. 4. Effect of HUP2976 on the GP-NPC1 interaction. ELISA plates were coated with thermolysin-treated VLPs, followed by incubation with HUP2976 or mAb114, HA-tagged NPC1 or mock cell lysates, a rat anti-HA antibody, and HRP-conjugated anti-rat IgG (H+L). The reaction was visualized with the TMB substrate. The OD values of mock cell lysates were subtracted from those of HUP2976- or mAb114-treated lysates at each concentration. The experiment was performed in triplicate and averages and standard deviations are shown.

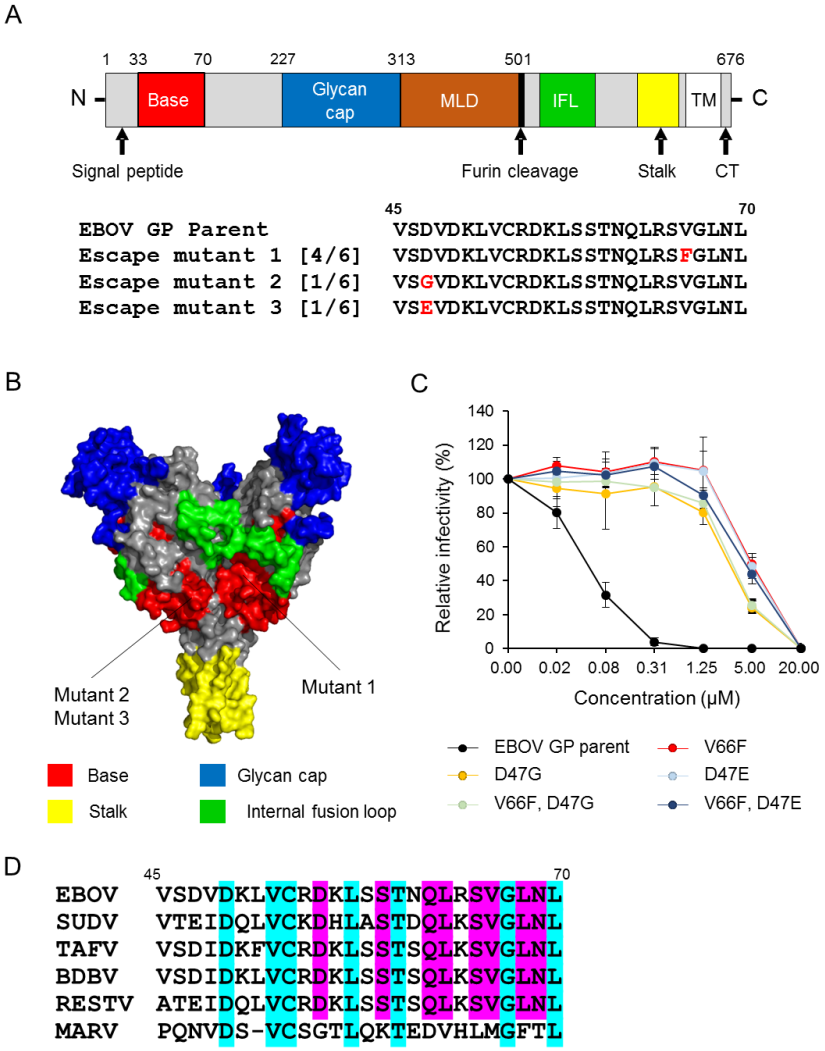

Fig. 5. Identification of amino acid substitutions allowing escape in EBOV GP. (A) The primary structure of GP and amino acid sequences at positions 45-70 are shown. The primary GP structure contains the base, glycan cap, mucin-like domain (MLD), internal fusion loop (IFL), and transmembrane region (TM) and cytoplasmic tail (CT). Amino acid substitutions found in the EBOV GP escape mutants selected under HUP2976 pressure are shown in red. (B) The trimeric structure of EBOV GP (PDB code: 6G95) was constructed using PyMOL 1.2r3pre (Schrödinger) and the colored corresponding sequence map above. (C) VSVs pseudotyped with wildtype and mutant EBOV GPs were diluted to 1,000 IU/ml, mixed with equal volumes of HUP2976, and inoculated onto Vero E6 cells. The cells were incubated at 37˚C for 18 hr, and GFP-expressing cells were counted with IN Cell Analyzer. Averages and standard deviations from 3 independent experiments are shown. (D) Amino acid sequences at positions 45-70 (EBOV numbering) of ebolavirus and marburgvirus GPs.

the inhibitory effect of HUP2976. However, it is worth noting that neither single nor multiple mutations in GP made the virus fully resistant to this compound. The amino acid residues at positions 47 and 66 mapped on the GP trimeric structure (PDB code: 5JQ3) revealed that the distance between Cα atoms of these two residues was 19.9 Å (in a GP monomer) in the base region of the chalice-like GP structure (Fig. 6). The distances from positions 47 to 47, from 66 to 66, and from 47 to 66 between the GP monomers were 37.8 Å, 33.3 Å, and 28.0 Å, respectively. Interestingly, D47 and V66 were located in the same cavity formed by 2 neighboring GP monomers (Fig. 6B).

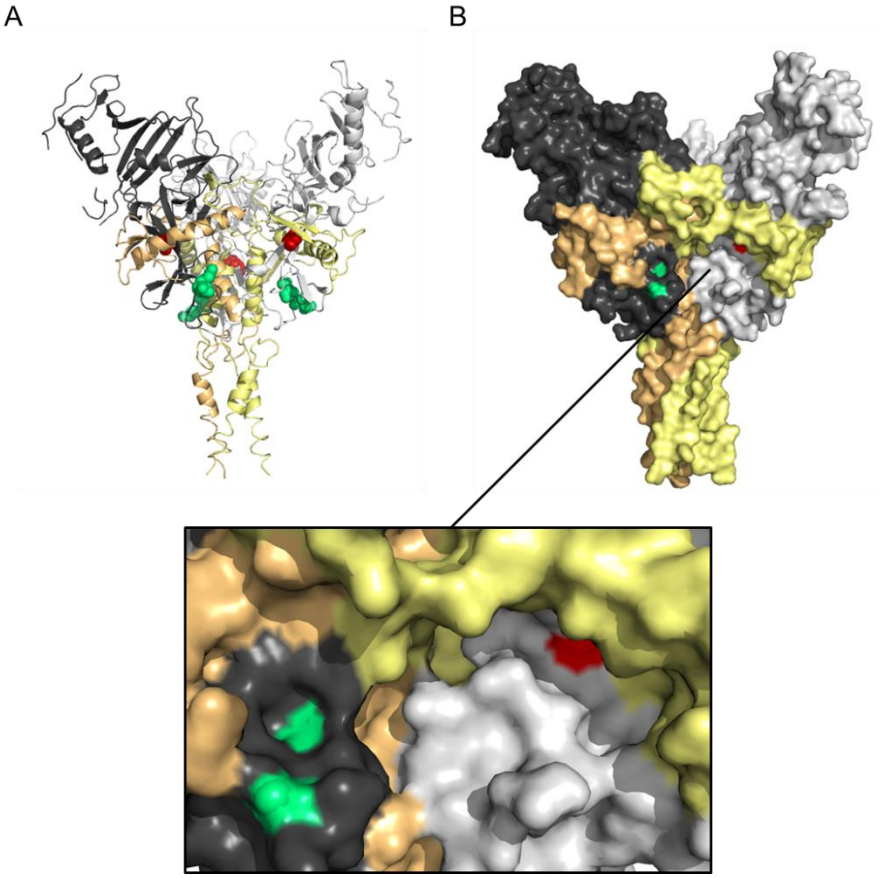

Fig. 6. Substituted amino acid residues mapped on the GP trimeric structure. The amino acid residues at positions 47 ad 66 are mapped on a ribbon model (A) and surface model (B) of the EBOV GP trimeric structure constructed using PyMOL 1.2r3pre (Schrödinger) based on the crystal structure (PDB code: 6G95). A close-up of the EBOV GP inhibitor-binding pocket in a surface representation in the solid black square. GP1 and GP2 are shown in black and orange in a GP monomer and in gray and yellow in another monomer, respectively. Green and red spheres represent D47 and V66 residues, respectively.

Discussion

During the epidemic of EVD in West Africa, favipiravir (T-705), a viral RNA polymerase inhibitor approved for conditional use to treat influenza infections in Japan, was investigated for treatment of EVD patients[30,47]. However, its therapeutic potency remains questionable due to the limited efficacy for patients with high EBOV titers. Other experimental drugs such as remdesivir have also been used in the latest outbreak in the DRC. All these chemical compound-based drug candidates are nucleotide analogues expected to interfere with the function of the viral RNA polymerase L. HUP2976 inhibits ebolavirus infection by blocking the entry of these viruses into cells. I found that HUP2976 had the potential to inhibit GP-mediated infection with VSV pseudotypes carrying GPs of representative members of all known human-pathogenic filovirus species. Notably, the inhibitory effects on EBOV GP- and BDBV GP-mediated infection were particularly strong. Our data suggest that HUP2976 may be a pan-filovirus therapeutic.

It was demonstrated that HUP2976 inhibited fusion between the endosomal membrane and viral envelope. It has been shown that low endosomal pH leads to proteolytic processing of filovirus GPs during the transport of filovirus particles to late endosomes, and the exposed receptor binding site of the proteolytically processed GP is thought to interact with NPC1, followed by membrane fusion[20,21]. Since the endosomal pH was not significantly changed in HUP2976-treated cells, it is unlikely that altered acidification conditions affected the viral infectivity. The fact that HUP2976 did not reduce the infectivity of VSVΔG*-G supports this notion. Thus, it was first hypothesized that HUP2976 inhibited the binding between GP and NPC1. However, contrary to our expectation, the binding of these molecules was not blocked by HUP2976. By analyzing the GP sequences of escape mutants, I found that amino acid residues D47 and V66 might

be important for the antiviral effects of HUP2976. These amino acid residues are well conserved among ebolaviruses and located in the base region (Fig. 5D), which seems to be important to form or stabilize the trimeric structure of GP.

Recently, selective estrogen receptor modulators (SERM), painkillers, antianginals antidepressants, and antipsychotics have been reported to have potential as fusion inhibitors against ebolaviruses[48–51]. While clomiphene, a SERM, blocks filovirus entry indirectly by affecting the function of NPC1[52], toremifene is thought to bind the GP molecule directly, to decrease its stability, and thus to prevent the fusion between the viral envelope and endosomal membrane. Interestingly, drugs such as toremifene, bepridil, paroxetine and sertraline seem to interact with V66 in the cavity on the GP surface (Fig. 6)[49,53]. It is conceivable that the interactions of inhibitors with the GP base involving V66 may affect the structural flexibility or stability of the GP molecule, resulting in reduced membrane fusion activity[50,53]. However other possible mechanisms caused by HUP2976 (e.g., cholesterol accumulation in endosomes and inhibitory effects on proteolytic cleavage of GP) are not ruled out.

Although direct evidence needs to be provided, escape mutations of amino acids D47 and V66 suggest that HUP2976 may directly interact with this cavity like other previously found fusion inhibitors such as toremifene, bepridil, paroxetine and sertraline. However, the amino acid comparison among filovirus GPs (Fig. 5D) suggests that D47 and V66 are not the only amino acids that are involved in the interaction between HUP2976 and GP. EBOV, BDBV, and TAFV GPs are identical at these positions but EBOV and BDBV GPs are more sensitive to HUP2976 than TAFV GP, and RESTV and SUDV GPs having E47 and V66 displayed differential sensitivities to HUP2976. Detailed molecular mechanisms of HUP2976-mediated fusion inhibition, including identification

of the amino acids responsible for the HUP2976-GP interaction, need to be clarified in future studies.

Although many entry inhibitors against EBOV such as ion channel blockers (e.g., amiodarone and bepridil), antimicrobials (e.g., amodiaquine and teicoplanin), psychoactive drugs (e.g., benztropine and imipramine), and protein kinase inhibitors (e.g., erlotinib and sunitinib) have been reported, none of them has been approved by the FDA for the treatment of EVD[54]. It has been reported that most of these drug candidates inhibit ebolavirus infection by affecting host intracellular factors such as NPC1, host protease cathepsin, calcium signaling required for endosomal fusion and so on. It should be considered that such compounds that may affect cellular functioins may have the potential to cause detrimental effects in clinical use. Although further studies are required, candidate compounds that interfere with GP function by direct interactions with the GP molecule may be promising candidates for the development of EVD drugs in the future.

Other viral proteins are also useful targets to develop EVD therapeutics. For example, NP, VP35, and VP24 play key roles in the life cycle of ebolaviruses by mediating nucleocapsid transport[55]. Inhibition of the functions of these proteins may reduce the replication efficiency of filoviruses. Indeed, it was reported that siRNA therapeutics targeting VP24 and VP35 might be one of the options as indicated by their efficacy in nonhuman primate models[56,57]. Interactions between VP40 and other host proteins may also be an interesting target. Further studies on drug design focusing on therapeutic agents that directly inhibit viral protein functions and/or interfere with viral-host protein interaction are needed.

Summary

Ebolaviruses and marburgviruses, members of the family *Filoviridae*, are known to cause fatal diseases often associated with hemorrhagic fever. Recent outbreaks of Ebola virus disease in West African countries and the DRC have made clear the urgent need for the development of therapeutics and vaccines against filoviruses. Using replication-incompetent VSV pseudotyped with the EBOV GP, a chemical compound library was screened to obtain new drug candidates that inhibit filoviral entry into target cells. I discovered a biaryl sulfonamide derivative that suppressed *in vitro* infection mediated by GPs derived from all known human-pathogenic filoviruses. To determine the inhibitory mechanism of the compound, each entry step (attachment, internalization, and membrane fusion) was monitored using lipophilic tracer-labeled VLPs and it was found that the compound efficiently blocked fusion between the viral envelope and the endosomal membrane during cellular entry. However, the compound did not block the interaction of GP with the NPC1 protein, which is believed to be the receptor of filoviruses. Using replication-competent VSVs pseudotyped with EBOV GP, escape mutants were selected and identified two EBOV GP amino acid residues (positions 47 and 66) important for the interaction with this compound. Interestingly, these amino acid residues were located at the base region of the GP trimer, suggesting that the compound might interfere with the GP conformational change required for membrane fusion. These results suggest that this biaryl sulfonamide derivative is a novel fusion inhibitor and a possible drug candidate for the development of a pan-filovirus therapeutic.

Chapter II:

Screening of chemical compounds that inhibit ebolavirus gene expression and egress from cells

The contents of this chapter will be submitted for publication in peer-reviewed journal, and thus cannot be shown in the thesis published online at the present time.

Abstract

Following the EVD outbreaks in Africa, there has been an increased necessity of effective therapies against EBOV. Several candidate drugs have been clinically tested until now but an antibody therapy has only been approved by FDA in 2020. Thus, more treatment options including chemical compound-based drugs for EVD are needed. This chapter focuses on chemical compounds for the development of anti-EBOV drugs, especially inhibitors of viral genome transcription/replication and budding. I screened a chemical compound library from ITbM and discovered several compounds that inhibited the EBOV minigenome-derived luciferase activity and/or the egress of virions. Here I discuss that EBOV replication and budding steps are good targets for therapeutic agents although such drugs have never been approved yet. Candidate compounds that were discovered in this study are expected to provide novel perspectives for the development of anti-EBOV drugs in the future.

Conclusion

Ebolaviruses are known as causative agents of EVD of human and nonhuman primates. EVD cases are reported sporadically in African countries. However, therapeutics against EVD are not sufficiently available although an antibody-based drug for the treatment of EVD, Inmazeb, has been approved by United States FDA in 2020. To seek novel candidates of anti-EVD drugs, I focused on small chemical compounds which have some advantages like cost effectiveness, easy storage conditions, long shelf life, and so on, compared to antibody therapeutics.

In chapter I, I described the antiviral potential and mechanisms of action of the compound, HUP2976, which has been identified as a novel EBOV entry inhibitor through screening using VSV pseudotyped with EBOV GP. The mechanism of the inhibition by the compound was determined: HUP2976 prevents fusion between viral membrane and endosomal membrane by interfering with the conformational change of the GP molecules, which is required for the membrane fusion followed by subsequent release of the RNP complex into cytoplasm. The discovery of this novel drug candidate is expected to contribute to the future development of EVD therapies.

In chapter II, I established plasmid-driven reporter and VLP formation assays to explore chemical compounds that inhibit EBOV gene replication and/or budding. Using these assays, a chemical compound library with approximately 20,000 compounds was screened for their inhibition potential of EBOV genome replication and budding. I discovered eleven replication inhibitors and twelve budding inhibitors from the compound library. Although further study for these compounds are needed, these findings, particularly the discovery of the compounds that affect EBOV budding, provide additional insights into the development of therapeutics against EVD.

This study aimed to search for better drug candidate compounds for the treatment of EVD and I discovered a novel entry inhibitor and several candidates for replication/budding inhibitors against EBOV. For the practical application of the compounds found in this study, further research is needed on specificity, cytotoxicity, structure-activity relationship, *in vivo* pharmacokinetics, combined use of multiple drugs with different antiviral mechanisms, and so on. Taken together, findings in this thesis are expected to contribute to the development of EVD therapeutics in the future.

Acknowledgments

I express my deepest gratitude to my supervisor, Prof. Ayato Takada (Division of Global Epidemiology, Research Center for Zoonosis Control, Hokkaido Univ., Sapporo, Japan), whose comments and suggestions were innumerably valuable throughout the course of my study. He also provided many opportunities for me to conduct field work abroad and participate in conferences.

I sincerely appreciate the invaluable support and advice provided by Prof. Hideaki Higashi (Division of Infection and Immunity, Research Center for Zoonosis Control, Hokkaido Univ., Sapporo, Japan), Prof. Hiroaki Kariwa (Laboratory of Public Health, Graduate School of Veterinary Medicine, Hokkaido Univ., Sapporo, Japan), Yoshihiro Sakoda (Laboratory of Microbiology, Graduate School of Veterinary Medicine, Hokkaido Univ., Sapporo, Japan), and Associate Prof. Manabu Igarashi (Division of Global Epidemiology, Research Center for Zoonosis Control, Hokkaido Univ., Sapporo, Japan) during my research work.

I am deeply grateful to Specially Appointed Assistant Prof. Reiko Yoshida, Specially Appointed Assistant Prof. Rashid Manzoor, Assistant Prof. Masahiro Kajihara (Division of Global Epidemiology, Research Center for Zoonosis Control, Hokkaido Univ., Sapporo, Japan) and Prof, Asuka Nanbo (The National Research Center for the Control and Prevention of Infectious Diseases, Nagasaki Univ., Nagasaki, Japan) for their technical and intellectual support.

I particularly thank Dr. Masahiro Sakaitani (Lilac Pharma. Co., Sapporo, Japan), Dr. Andrea Marzi, and Dr. Heinz Feldmann (Laboratory of Virology, Division of Intramural Research, National Institute of Allergy and Infectious Diseases, National Institutes of Health, Hamilton, Montana, United States of America) for their thoughtful

advice and cooperation. Working with them proved to be a truly valuable experience.

I am grateful to the coordinator of the Program for Leading Graduate Schools, Hokkaido Univ., Prof. Motohiro Horiuchi (Laboratory of Veterinary Hygiene, Graduate School of Veterinary Medicine, Hokkaido Univ., Sapporo, Japan), and the members of the Leading Program Office for their help with my PhD coursework.

I thank Dr. Masahiro Sato, Dr. Yoshihiro Takadate, and Ms. Hiroko Miyamoto (Division of Global Epidemiology, Research Center for Zoonosis Control, Hokkaido Univ.) for their advice and suggestions.

I wish to specially thank my friend, Dr. Satoshi Ito for his encouragement and emotional support. Finally, I express my gratitude to my family, Mitsuko Isono and Coco Isono for their understanding, love, and daily generous support.

和文要旨

フィロウイルス科に属するエボラウイルスおよびマールブルグウイルスは、ヒトを含む霊長類に高い致死率を伴う出血熱を引き起こす人獣共通感染症病原体の一つである。近年、大規模なエボラウイルス病（EVD）のアウトブレイクがアフリカ地域を中心に報告されている。2013 年から 2016 年にかけて西アフリカで発生した EVD の未曾有の大流行および 2018 年から 2020 年のコンゴ民主共和国での流行の際に、EVD に対する様々な治療薬の臨床試験が行われ、2020 年 10 月に抗体医薬による初めての抗エボラウイルス薬 Inmazeb が承認された。しかし、この抗体医薬品は生産コストが高い上に、使用上の問題から投与できない患者も一定数想定される。一方、これまでにファビピラビルやレムデジビルに代表される核酸類似体が、エボラウイルスのゲノム複製阻害薬の候補化合物として報告されてきたが、実用化には至っていないため、さらなる安価で安全な EVD 治療薬の開発が求められている。

第一章では、エボラウイルスの表面糖タンパク質（GP）を纏ったシュードタイプウイルスを用いて、既存の化合物ライブラリーからフィロウイルスの細胞侵入を阻害する治療薬候補化合物として見つかった HUP2976 の解析を行った。共焦点顕微鏡を用いて、蛍光標識したエボラウイルス様粒子（VLP）の細胞侵入過程（吸着・取り込み・膜融合）を HUP2976 存在下および非存在下で比較した結果、本化合物は粒子がエンドソーム内に取り込まれた後の膜融合を阻害していることが示唆された。エボラウイルスの膜融合は、エンドソーム内に存在する膜融合レセプターである Niemann-Pick C1 (NPC1)蛋白質と GP の相互作用を介して引き起こされると考えられているが、HUP2976 は NPC1 と GP の結合を阻害しなかった。次に、増殖性シュードタイプウイルスを用いたエスケープミュータントを選択し、アミノ酸配列を解析したところ、GP 分子上の基幹部位に変異が見つかり、その変異箇所が HUP2976 の作用部位である事が示唆された。これらの結果は、HUP2976 はエボラウイルスの GP 分子に直接作用して構造変化を抑制

し、エンドソーム膜とウイルスエンベロープの膜融合を阻害することで、エボラウイルスの細胞侵入阻害活性を示すことを示唆している。

第二章では、エボラウイルスの細胞内増殖過程のうち、細胞侵入以外のステップ、すなわちゲノム転写・複製および出芽過程を標的とした新たな治療薬候補化合物の探索を試みた。まず、エボラウイルスゲノムにコードされている 7 つのタンパク質、レポーター遺伝子としてルシフェラーゼをコードするエボラウイルスミニゲノムおよび T7 プロモーターを発現するプラスミドを細胞に導入し、細胞内に発現したルシフェラーゼおよび培養上清中に産生される VLP 量を検出することによって、エボラウイルスゲノムの転写・複製および出芽を同時に評価できる実験系を確立した。この評価系をもとに、約 20,000 化合物のスクリーニングを行った結果、転写・複製阻害活性を持つ化合物を 11 個および出芽阻害活性を持つ化合物を 12 個見いだした。そのうち、転写・複製および出芽の両方に阻害活性を示したものは 7 個であった。

本研究は、EVD に対する新規治療薬候補化合物を探索することを目的として行った。現在唯一の承認薬である Inmazeb に代表される抗体医薬に比べ、生産コストならびに保管の簡便さや効能成分の安定性などの面で優位である低分子化合物は、EVD が問題となる地域であるアフリカで、より理想的な薬剤であると考えられる。本研究で見つかった化合物の実用化に向けて、選択性、細胞毒性、構造活性相関および生体内での薬物動態等についてさらなる研究が必要であるが、得られた知見は今後の EVD 治療薬の開発に貢献することが期待される。

References

1. Sahul Hameed, A. S., Ninawe, A. S., Nakai, T., Chi, S. C. & Johnson, K. L. ICTV virus taxonomy profile: *Filoviridae. J. Gen. Virol.* **100**, 911–912 (2019).
2. Goldstein, T. *et al.* The discovery of Bombali virus adds further support for bats as hosts of ebolaviruses. *Nat. Microbiol.* **3**, 1084–1089 (2018).
3. Rollin, P. E. *et al.* Ebola (Subtype Reston) Virus among Quarantined Nonhuman Primates Recently Imported from the Philippines to the United States. *J. Infect. Dis.* **179**, S108–S114 (1999).
4. Emanuel, J., Marzi, A. & Feldmann, H. Filoviruses: Ecology, Molecular Biology, and Evolution. *Adv. Virus Res.* **100**, 189–221 (2018).
5. Mbala-Kingebeni, P. *et al.* Medical countermeasures during the 2018 Ebola virus disease outbreak in the North Kivu and Ituri Provinces of the Democratic Republic of the Congo: a rapid genomic assessment. *Lancet Infect. Dis.* **3099**, 1–10 (2019).
6. Mbala-Kingebeni, P. *et al.* 2018 Ebola virus disease outbreak in Équateur Province, Democratic Republic of the Congo: a retrospective genomic characterisation. *Lancet Infect. Dis.* **3099**, 1–7 (2019).
7. Tariq, A., Roosa, K., Mizumoto, K. & Chowell, G. Assessing reporting delays and the effective reproduction number: The Ebola epidemic in DRC, May 2018–January 2019. *Epidemics* **26**, 128–133 (2019).
8. WHO. Ebola | Ebola situation reports: Democratic Republic of the Congo. *WHO* (2020). doi:https://www.who.int/ebola/situation-reports/drc-2018/en/
9. World Health Organization. Ebola in the Democratic Republic of the Congo 2020 - Équateur Province. (2020).

doi:https://www.who.int/emergencies/diseases/ebola/ebola-health-update---équateur-province-democratic-republic-of-the-congo-2020

10. FDA. Drug Trials Snapshots: INMAZEB | FDA. *FDA* (2020). doi:https://www.fda.gov/drugs/drug-approvals-and-databases/drug-trials-snapshots-inmazeb
11. Hunt, C. L., Lennemann, N. J. & Maury, W. Filovirus entry: A novelty in the viral fusion world. *Viruses* **4**, 258–275 (2012).
12. Takada, A. *et al.* A system for functional analysis of Ebola virus glycoprotein. *Proc. Natl. Acad. Sci.* **94**, 14764–9 (1997).
13. Alvarez, C. P. *et al.* C-Type Lectins DC-SIGN and L-SIGN Mediate Cellular Entry by Ebola Virus in cis and in trans . *J. Virol.* **76**, 6841–6844 (2002).
14. Kondratowicz, A. S. *et al.* T-cell immunoglobulin and mucin domain 1 (TIM-1) is a receptor for Zaire Ebolavirus and Lake Victoria Marburgvirus. *Proc. Natl. Acad. Sci.* **108**, 8426–8431 (2011).
15. Takada, A. *et al.* Human macrophage C-type lectin specific for galactose and N-acetylgalactosamine promotes filovirus entry. *J. Virol.* **78**, 2943–7 (2004).
16. Nanbo, A. *et al.* Ebolavirus Is Internalized into Host Cells via Macropinocytosis in a Viral Glycoprotein-Dependent Manner. *PLoS Pathog.* **6**, e1001121 (2010).
17. Saeed, M. F., Kolokoltsov, A. A., Albrecht, T. & Davey, R. A. Cellular entry of ebola virus involves uptake by a macropinocytosis-like mechanism and subsequent trafficking through early and late endosomes. *PLoS Pathog.* **6**, e1001110 (2010).
18. Bhattacharyya, S. *et al.* Ebola virus uses clathrin-mediated endocytosis as an entry pathway. *Virology* **401**, 18–28 (2010).

19. Schornberg, K. *et al.* Role of Endosomal Cathepsins in Entry Mediated by the Ebola Virus Glycoprotein. *J. Virol.* **80**, 4174–4178 (2006).

20. Carette, J. E. *et al.* Ebola virus entry requires the cholesterol transporter Niemann-Pick C1. *Nature* **477**, 340–343 (2011).

21. Côté, M. *et al.* Small molecule inhibitors reveal Niemann-Pick C1 is essential for Ebola virus infection. *Nature* **477**, 344–348 (2011).

22. Basler, C. F. *et al.* The Ebola virus VP35 protein functions as a type I IFN antagonist. *Proc. Natl. Acad. Sci.* **97**, 12289–12294 (2000).

23. Zhang, A. P. P. *et al.* The ebolavirus VP24 interferon antagonist: Know your enemy. *Virulence* **3**, 440–445 (2012).

24. Jasenosky, L. D. & Kawaoka, Y. Filovirus budding. *Virus Res.* **106**, 181–188 (2004).

25. Noda, T. *et al.* Ebola Virus VP40 Drives the Formation of Virus-Like Filamentous Particles Along with GP. *J. Virol.* **76**, 4855–4865 (2002).

26. The PREVAIL II Writing Group. A Randomized, Controlled Trial of ZMapp for Ebola Virus Infection. *N. Engl. J. Med.* **375**, 1448–1456 (2016).

27. WHO. Ebola | Ebola treatments approved for compassionate use in current outbreak. *WHO* (2018). doi:https://www.who.int/ebola/drc-2018/treatments-approved-for-compassionate-use/en/

28. Cardile, A. P., Downey, L. G., Wiseman, P. D., Warren, T. K. & Bavari, S. Antiviral therapeutics for the treatment of Ebola virus infection. *Curr. Opin. Pharmacol.* **30**, 138–143 (2016).

29. Nakkazi, E. Randomised controlled trial begins for Ebola therapeutics. *Lancet* **392**, 2338 (2018).

30. Sissoko, D. *et al.* Experimental Treatment with Favipiravir for Ebola Virus Disease (the JIKI Trial): A Historically Controlled, Single-Arm Proof-of-Concept Trial in Guinea. *PLoS Med.* **13**, 1–36 (2016).

31. NIH. Clinical Trial of Investigational Ebola Treatments Begins in the Democratic Republic of the Congo | NIH: National Institute of Allergy and Infectious Diseases. (2019). doi:https://www.niaid.nih.gov/news-events/clinical-trial-investigational-ebola-treatments-begins-democratic-republic-congo

32. Aleksandrowicz, P. *et al.* Ebola virus enters host cells by macropinocytosis and clathrin-mediated endocytosis. *J. Infect. Dis.* **204**, 957–967 (2011).

33. Ng, M. *et al.* Cell entry by a novel European filovirus requires host endosomal cysteine proteases and Niemann-Pick C1. *Virology* **468**, 637–646 (2014).

34. Kondoh, T. *et al.* Single-Nucleotide Polymorphisms in Human NPC1 Influence Filovirus Entry Into Cells. *J. Infect. Dis.* **218**, S397–S402 (2018).

35. Furuyama, W., Miyamoto, H., Yoshida, R. & Takada, A. Quantification of filovirus glycoprotein-specific antibodies. *Methods Mol. Biol.* **1628**, 309–320 (2017).

36. Nakayama, E. *et al.* Antibody-dependent enhancement of marburg virus infection. *J. Infect. Dis.* **204**, (2011).

37. Takada, A. *et al.* Identification of Protective Epitopes on Ebola Virus Glycoprotein at the Single Amino Acid Level by Using Recombinant Vesicular Stomatitis Viruses. *J. Virol.* **77**, 1069–1074 (2003).

38. Ebihara, H. *et al.* In Vitro and In Vivo Characterization of Recombinant Ebola Viruses Expressing Enhanced Green Fluorescent Protein. *J. Infect. Dis.* **196**, S313–S322 (2007).

39. Furuyama, W. *et al.* Discovery of an antibody for pan-ebolavirus therapy. *Sci. Rep.* **6**, 20514 (2016).

40. Miller, E. H. *et al.* Ebola virus entry requires the host-programmed recognition of an intracellular receptor. *EMBO J.* **31**, 1947–1960 (2012).

41. Cagigi, A. *et al.* Vaccine Generation of Protective Ebola Antibodies and Identification of Conserved B-Cell Signatures. *J. Infect. Dis.* **218**, S528–S536 (2018).

42. Saito, S. *et al.* IgA tetramerization improves target breadth but not peak potency of functionality of anti-influenza virus broadly neutralizing antibody. *PLoS Pathog.* **15**, 1–23 (2019).

43. Tiller, T. *et al.* Efficient generation of monoclonal antibodies from single human B cells by single cell RT-PCR and expression vector cloning. *J. Immunol. Methods* **329**, 112–24 (2008).

44. Kuroda, M. *et al.* Interaction between TIM-1 and NPC1 Is Important for Cellular Entry of Ebola Virus. *J. Virol.* **89**, 6481–6493 (2015).

45. Misasi, J. *et al.* Structural and molecular basis for Ebola virus neutralization by protective human antibodies. *Science (80-.).* **351**, 1343–1346 (2016).

46. King, L. B., West, B. R., Schendel, S. L. & Saphire, E. O. The structural basis for filovirus neutralization by monoclonal antibodies. *Curr. Opin. Immunol.* **53**, 196–202 (2018).

47. Bai, C. Q. *et al.* Clinical and Virological Characteristics of Ebola Virus Disease Patients Treated with Favipiravir (T-705) - Sierra Leone, 2014. *Clin. Infect. Dis.* **63**, 1288–1294 (2016).

48. Johansen, L. M. *et al.* A screen of approved drugs and molecular probes

identifies therapeutics with anti-Ebola virus activity. *Sci. Transl. Med.* **7**, 290ra89 (2015).

49. Zhao, Y. *et al.* Toremifene interacts with and destabilizes the Ebola virus glycoprotein. *Nature* **535**, 169–172 (2016).

50. Shaikh, F. *et al.* Structure-based In Silico Screening Identifies a Potent Ebolavirus Inhibitor from a Traditional Chinese Medicine Library. *J. Med. Chem.* **62**, 2928–2937 (2019).

51. Zhao, Y. *et al.* Structures of Ebola Virus Glycoprotein Complexes with Tricyclic Antidepressant and Antipsychotic Drugs. *J. Med. Chem.* **61**, 4938–4945 (2018).

52. Shoemaker, C. J. *et al.* Multiple Cationic Amphiphiles Induce a Niemann-Pick C Phenotype and Inhibit Ebola Virus Entry and Infection. *PLoS One* **8**, e56265 (2013).

53. Ren, J., Zhao, Y., Fry, E. E. & Stuart, D. I. Target Identification and Mode of Action of Four Chemically Divergent Drugs against Ebolavirus Infection. *J. Med. Chem.* **61**, 724–733 (2018).

54. Salata, C. *et al.* Ebola Virus Entry: From Molecular Characterization to Drug Discovery. *Viruses* **11**, 274 (2019).

55. Takamatsu, Y., Kolesnikova, L. & Becker, S. Ebola virus proteins NP, VP35, and VP24 are essential and sufficient to mediate nucleocapsid transport. *Proc. Natl. Acad. Sci.* **115**, 1075–1080 (2018).

56. Geisbert, T. W. *et al.* Postexposure protection of non-human primates against a lethal Ebola virus challenge with RNA interference: a proof-of-concept study. *Lancet* **375**, 1896–1905 (2010).

57. Warren, T. K. *et al.* Advanced antisense therapies for postexposure protection

against lethal filovirus infections. *Nat. Med.* **16**, 991–994 (2010).

58. Cardile, A. P., Downey, L. G., Wiseman, P. D., Warren, T. K. & Bavari, S. Antiviral therapeutics for the treatment of Ebola virus infection. *Curr. Opin. Pharmacol.* **30**, 138–143 (2016).

59. Mulangu, S. *et al.* A Randomized, Controlled Trial of Ebola Virus Disease Therapeutics. *N. Engl. J. Med.* **381**, 2293–2303 (2019).

60. Watanabe, S., Noda, T., Halfmann, P., Jasenosky, L. & Kawaoka, Y. Ebola virus (EBOV) VP24 inhibits transcription and replication of the EBOV genome. *J. Infect. Dis.* **196 Suppl**, S284–S290 (2007).

61. Niwa, H., Yamamura, K. & Miyazaki, J. Efficient selection for high-expression transfectants with a novel eukaryotic vector. *Gene* **108**, 193–199 (1991).

62. Raymond, C. *et al.* A simplified polyethylenimine-mediated transfection process for large-scale and high-throughput applications. *Methods* **55**, 44–51 (2011).

63. Watanabe, S. *et al.* Production of Novel Ebola Virus-Like Particles from cDNAs : an Alternative to Ebola Virus Generation by Reverse Genetics. *J. Virol.* **78**, 999–1005 (2004).

64. Cardile, A. P., Warren, T. K., Martins, K. A., Reisler, R. B. & Bavari, S. Will there be a cure for Ebola? *Annu. Rev. Pharmacol. Toxicol.* **57**, 329–348 (2017).

65. Cross, R. W., Mire, C. E., Feldmann, H. & Geisbert, T. W. Post-exposure treatments for Ebola and Marburg virus infections. *Nat. Rev. Drug Discov.* **17**, 413–434 (2018).

66. Warren, T. K. *et al.* Therapeutic efficacy of the small molecule GS-5734 against Ebola virus in rhesus monkeys. *Nature* **531**, 381–385 (2016).

67. Shiraki, K. & Daikoku, T. Favipiravir, an anti-influenza drug against life-

threatening RNA virus infections. *Pharmacol. Ther.* **209**, 107512 (2020).

68. Lo, M. K. *et al.* GS-5734 and its parent nucleoside analog inhibit Filo-, Pneumo-, and Paramyxoviruses. *Sci. Rep.* **7**, 1–7 (2017).

69. Licata, J. M., Johnson, R. F., Han, Z. & Harty, R. N. Contribution of Ebola Virus Glycoprotein, Nucleoprotein, and VP24 to Budding of VP40 Virus-Like Particles. *J. Virol.* **78**, 7344–7351 (2004).

70. Kajihara, M. *et al.* Inhibition of Marburg Virus Budding by Nonneutralizing Antibodies to the Envelope Glycoprotein. *J. Virol.* **86**, 13467–13474 (2012).

71. Hoenen, T., Groseth, A. & Feldmann, H. Therapeutic strategies to target the Ebola virus life cycle. *Nat. Rev. Microbiol.* **17**, 593–606 (2019).

72. Nicholson, K. G. *et al.* Efficacy and safety of oseltamivir in treatment of acute influenza: A randomised controlled trial. *Lancet* **355**, 1845–1850 (2000).

73. Treanor, J. J. *et al.* Efficacy and safety of the oral neuraminidase inhibitor oseltamivir in treating acute influenza: A randomized controlled trial. *J. Am. Med. Assoc.* **283**, 1016–1024 (2000).

74. Noda, T. *et al.* Assembly and budding of Ebolavirus. *PLoS Pathog.* **2**, 0864–0872 (2006).

75. Licata, J. M. *et al.* Overlapping Motifs (PTAP and PPEY) within the Ebola Virus VP40 Protein Function Independently as Late Budding Domains: Involvement of Host Proteins TSG101 and VPS-4. *J. Virol.* **77**, 1812–1819 (2003).

76. Martin-Serrano, J., Zang, T. & Bieniasz, P. D. HIV-1 and Ebola virus encode small peptide motifs that recruit Tsg101 to sites of particle assembly to facilitate egress. *Nat. Med.* **7**, 1313–1319 (2001).

77. Han, Z. *et al.* ITCH E3 Ubiquitin Ligase Interacts with Ebola Virus VP40 To

Regulate Budding. *J. Virol.* **90**, 9163–9171 (2016).

78. Harty, R. N., Brown, M. E., Wang, G., Huibregtse, J. & Hayes, F. P. A PPxY motif within the VP40 protein of Ebola virus interacts physically and functionally with a ubiquitin ligase: Implications for filovirus budding. *Proc. Natl. Acad. Sci. U. S. A.* **97**, 13871–13876 (2000).

79. Nanbo, A. & Ohba, Y. Budding of Ebola Virus Particles Requires the Rab11-Dependent Endocytic Recycling Pathway. in *Journal of Infectious Diseases* **218**, S388–S396 (2018).